Available online at www.sciencedirect.com
SCIENCE DIRECT
Polymer 47 (2006) 5392–5401
polymer
www.elsevier.com/locate/polymer

Morphological effects on glass transition behavior in selected immiscible blends of amorphous and semicrystalline polymers

Vivek Thirtha, Richard Lehman *, Thomas Nosker

Department of Materials Science and Engineering, AMIPP Advanced Polymer Center, Rutgers University, 607 Taylor Road, Piscataway, NJ 08854, USA

Received 13 February 2006; received in revised form 7 May 2006; accepted 8 May 2006

Abstract

The effects uncompatibilized immiscible polymer blend compositions on the T_g of the amorphous polymer were studied in the systems polystyrene/polypropylene (PS/PP), polystyrene/high density polyethylene (PS/PE) and polycarbonate/high density polyethylene (PC/PE). In the two similar systems of PS/PP and PS/PE, the T_g of PS increased with decreasing PS percentage in the blends. This variation in glass transition is attributed to the polymer domain interactions resulting from the different morphologies of various blend compositions. Experiments were conducted to study these effects by preparing blends with various polymers that varied the relationship between the T_g of the amorphous polymer and the crystallization behavior of the semicrystalline polymer. Results show that the variation in amorphous component T_g with composition depends strongly on the physical state of the semicrystalline domains. Whereas the T_g of PS in PS/PE blends changed with composition, the T_g of PC in the PC/PE blend did not change with composition.

Keywords: Blends; Glass transition; Morphology

1. Introduction

The ever-increasing demand for polymer materials with designed multifunctional properties has led to a diversity of blend development efforts that seek proportional as well as synergistic properties from combinations of known polymer materials [1]. Many polymer pairs are immiscible due to their high molecular weight and the consequent entropy constraints. Various techniques exist to compatibilize polymer pairs through interfacial modifications or copolymer addition, though these add cost to the blend. Alternatively, melt blending of uncompatibilized immiscible polymers can yield rule of mixtures behavior and in some cases synergism of properties at certain compositions [2–4]. Even though there is lack of chemical interaction between the components in an immiscible blend, the fine micron scale morphology obtained through melt blending is capable of affecting individual component transitions, such as crystallization and glass transition, through physical interactions.

Some aspects of the glass transition are still not well understood [5] and one of the more perplexing phenomena is the apparent dependence of glass transition on the size and morphology of a domain. Adam and Gibbs explained local relaxation based on the temperature dependence of the size of polymer domains called cooperatively rearranging regions (CRRs), which are several nanometers in size during the glass transition [6]. Jackson and McKenna observed that pore sizes of 73 nm in confined pore glasses changed the glass transition in a 'fundamental way', subsequently decreasing the T_g of *o*-terphenyl and benzoyl in these confined pores [7]. Decreases in T_g values have been observed in ultra thin freely standing polymer films. This is attributed to the free surface of the polymers, allowing a high percentage of polymer chains having unrestricted motion, thus reducing the thermal activation required for the glass transition [8,9]. When similar films were deposited on a substrate, the T_g increased due to the interaction or pinning of the surface polymer chains. A 50 °C increase in T_g of ultra-thin films of P(2)VP due to favorable interactions between films and substrates was observed [10]. This increase was due to the creation of an immobilized zone of polymer chains from the substrate interface, leading into the bulk.

Pronounced increases [11] and reductions [12,13] in T_g have been observed in systems filled with nanometer sized particles, due to the large amount of new surface area created by these

* Corresponding author. Tel.: +1 609 203 2501; fax: +1 732 445 5584.
E-mail address: rllehman@rutgers.edu (R. Lehman).

0032-3861/$ - see front matter © 2006 Elsevier Ltd. All rights reserved.
doi:10.1016/j.polymer.2006.05.014

particles in the polymer matrix [14]. An increase in the glass transition of polymers melt blended with micron scale inorganic fillers has been observed by several investigators. Such behavior has been observed in polypropylene (~3 °C at 20 wt% and ~7 °C at 48 wt%) by Yuan et al. and in Nylon 6 (~7 °C at 15 vol% and ~12 °C at 40 vol%) by Huang et al. when they are blended with glass beads having coupling agents on the surface [15,16]. Ilsaka and Shibayama showed a composition dependent increase in the T_g of polystyrene and polymethylmethacrylate blended with glass beads and mica particles dispersed in the polymer matrix, using DMA [17]. These observations were also attributed to the creation of an immobilized interfacial layer starting at the glass bead surface and extending a certain distance into the matrix. From the aforementioned work, the phase interfaces and the domain morphologies that result from particulate polymer composites or from extremely small polymer domains in free space, e.g. fibers and films, are clearly seen to play a large role in determining the properties of these materials. Since, uncompatibilized immiscible polymer blends have fine domains, usually at the micron scale, and a significant amount of non-bonded interface, the domains in such blends exhibit interfacial and domain size related effects similar to those referenced above.

Glass transition shifts in polymer blends are most generally observed due to partial or complete miscibility, though there have been some T_g changes observed based solely on morphology and physical interactions. The T_g of *a*PS was reported to change in blends with *i*PP by Mucha and attributed to the interface interactions between the components [18]. Reinsch and Rebenfeld reported an increase in the T_g of PET in PET/PC blends. They attributed this increase to the presence of a rigid, glassy polycarbonate matrix domain when PET goes through its glass transition, which causes the T_g to increase due to a friction at the interface/wall between the two phases [19]. The T_g of PP in PS/PP blends and the T_g of polybutadiene in a polystyrene matrix were shown to decrease with increasing PS concentration, an effect attributed to the negative pressure/diluency arising from differential thermal expansion coefficients [20,21].

We have shown in some of our earlier work that the glass transition of the individual polymers in immiscible blends can be affected by blend morphology [22]. T_g of PS in a PS–PP blend was increased with the decrease in PS composition, and observed to be dependent on the blend morphology. Such interface and domain size effects are also reflected in other common properties of the polymer such as the crystallization behavior, degree of crystallinity and the spherulite size, and the crystallization and melting temperatures [23–26]. A good example of these effects is the reduction in crystallization temperature observed at low PP concentrations in PS/PP blends [22,27].

In the present study, these glass transition effects in PS/PP blends have been reproduced with raw materials of higher purity compared to the previously published data. In addition, the concept that domain morphology strongly influences thermal transition behavior is further extended by investigating these effects on the T_g of individual components in the similar blends of PS/PE and PC/PE. The selection of these two blend systems provided an important degree of contrast in that the T_g of the amorphous polymer varied from less than to greater than the crystallization temperature of semicrystalline polymer as represented by the PS/PE and PC/PE systems, respectively. Thus, the effect of the physical state of PE during the glass transition of the amorphous polymer (PS and PC) was studied.

2. Experimental

2.1. Materials and processing

Polystyrene (PS), polypropylene (PP) and high density polyethylene (PE) were obtained from Aldrich Chemicals. Polycarbonate (PC) was supplied by GE Polymerland. The important properties of the materials are shown in Table 1. All materials were free of industrial additives or processing aids.

Blend compositions ranging from 20/80 to 90/10 (wt/wt) for PS/PE and 15/85 to 90/10 (wt/wt) for PS/PP, were compounded by melt blending in a single screw extruder (Brabender Intellitorque Plasti-corder). Cylindrical blend specimens were extruded with a 25:1 metering single screw having a diameter of 19 mm with mixing elements and a 13 mm die. While processing the PS/PP and PS/PE blends the temperatures in the three zones and the die were maintained at 220 °C and the screw speed was maintained at 50 rpm. These zone temperatures were increased to 260 °C while compounding the PC/PE blends, as the maximum torque capacity of the extruder was exceeded due to the high viscosity and high T_g of polycarbonate. For the PC/PE blends, compositions ranging from 20/80 to 90/10 (wt/wt) were prepared.

Rectangular solid samples required for the DMA analysis of these blends were processed using injection molding. A Negri-Bossi V55-200 molding machine was used and the processing temperatures were similar to those used during extrusion. A full range of compositions were injection molded for all the blends.

Table 1
Materials and properties

Material	Supplier	Product	Molecular weight (M_w)	Melt index (g/10 min)	Density	Viscosity (Pa s); (shear rate; 39 s^{-1})
Polystyrene (PS)	Aldrich	182427	280,000	3.16 (200 °C; 5.0 kg)	1.047	1211 (220 °C)
Polypropylene (PP)	Aldrich	427861	340,000	4.00 (230 °C; 2.16 kg)	0.900	1054 (220 °C)
High density polyethyene (PE)	Aldrich	427969	–	4.00 (190 °C; 2.16 kg)	0.946	1054 (220 °C) 1490 (260 °C)
Polycarbonate (PC)	GE polymerland	PK2870	–	2.5 (300 °C; 1.20 kg)	1.20	1490 (260 °C)

2.2. Rheology

To identify the phase inversion composition in these blends, rheological properties of the PS, PP, PC and PE were characterized by a stress controlled AR-2000 rheometer. A parallel plate geometry having a 25 mm diameter, with a gap of 1.0 mm between the plates was used for the experiment and polymer samples compression molded into disks were used. Linear viscoelastic regions (LVR) of the individual samples were selected based on stress sweeps and polymer melts were sheared in oscillation at a strain of 4% (PE), 2% (PC) and 3% (PS, PP). Frequency sweep experiments from 100 to 0.01 Hz were performed at the respective processing temperatures and the Cox–Merz transformation was applied on individual polymers to obtain shear-rate as a function of viscosity. Approximate co-continuous compositions were generated by equating the composition ratios to the viscosity ratios (data from Table 1) at shear rates determined by the rotational speed (50 rpm, 5.2 rad s^{-1}, shear rate = 39 s^{-1}).

2.3. Thermal transition characterization—MDSC and DMA

The thermal transitions of the blend components were studied using a Q1000 differential scanning calorimeter (TA Instruments, New Castle, DE) operated in modulated DSC mode (MDSC). Disk shaped samples, weighing approximately 12 mg were sliced from the extruded rod. DSC runs were conducted over the temperature range of 30–200 °C for the PS/PE blends, −40–220 °C for PS/PP blends, while for the PC/PE blends it was from 40 to 240 °C. A three part sequence that included modulated heat, cool and modulated reheat was employed, with an underlying heating and cooling rate of 3 °C/min, modulation amplitude of ±1.3 °C, with a period of 40 s. The reversing heat curve obtained by modulating the heating rate in the DSC was used for the T_g observation. Precise T_g values were assigned by measuring peaks on the derivative graph of the enthalpy versus temperature curve. This method reduces error associated with T_g measurements using the onset-end intercept method. Indium and sapphire standards were used to calibrate the DSC and an inert nitrogen atmosphere was maintained during the experiments. A refrigerated cooling system (RCS) was connected to the DSC to attain the lower temperatures used in the thermal analysis of PS/PP blends. Experimental variability was assessed through sixfold replication comprised of threefold sample replication (repeated blend preparation and processing) and twofold analytical replication (DSC heat and reheat). Appropriate statistical methods were used to generate least-significant-differences and corresponding errors bars for the comparison of experimental mean values.

Dynamic mechanical analysis was performed with an AR-2000 rheometer (TA Instruments, New Castle, DE), operated in the rectangular solid torsion mode inside an environmental test chamber. The test sample dimensions were approximately 50.0×13.0×3.5 mm. The samples were tested from −150 and 175 °C. Since, the test involved a wide temperature range and involved different sample gripping torques, the testing was divided into two parts: −150–25 °C and 25–175 °C. Samples were heated at a temperature rate of 2 °C/min at a frequency of 1 Hz. Liquid nitrogen was used to achieve the low temperatures and was also used to precisely control temperatures during heating. The strains for the linear viscoelastic region (LVR) of each sample were determined before the temperature ramp tests, and were found to be between 0.01 and 0.03%. The maxima of the G'' curves were used as the measure of glass transition temperature.

2.4. Microscopy

Specimens were fractured perpendicular to the extrusion axis in liquid nitrogen after 30 min of thermal equilibration to generate SEM specimens for morphological analysis. These specimens were sputter-coated with gold–palladium to prevent electron charging. PS/PE and PS/PP samples with PS composition less than 50% were etched with toluene to produce better image contrast. A Leo–Zeiss field emission scanning electron microscope was utilized to examine the specimens and record micrographs. During electron microscope imaging, the entire surface of each specimen was surveyed to assess uniformity of the blend, and micrographs were taken of representative areas. Overall, the samples were homogeneous and little difference could be discerned over the entire cross-section.

3. Results and discussion

3.1. PS–PE and PS–PP blends

3.1.1. Morphology

The micrographs in Fig. 1 show the representative cross-sectional morphologies of the PS/PE blends at various compositions. The 20% PS (Fig. 1(a)) and 35% PS (Fig. 1(b)) structures reveal a PE matrix with a dispersed PS phase. The PS domain morphology in these images is represented by the dark etched (PS removed) regions. The PS in the 20PS/80PE blend is finely dispersed in globules with sizes varying from 300 nm to 2.5 μm and an average size of 1.1 μm. As the PS concentration is increased to 35%, either the number of dispersed PS globules must increase at nearly constant diameter or the PS will coalesce to produce larger domains with a proportional adjustment in their number. The morphology that results depends on the competing processes of droplet break up and coalescence. Although clearly droplet breakup is the dominant effect under the high shear field of the extruder, both processes occur and a sort of equilibrium is established between these processes based on the interfacial surface energy and the applied shear rate [28]. As seen in Fig. 1, the 20/80 composition illustrates finely dispersed structure that clearly indicates a predominance of droplet breakup, whereas the 35/65 composition shows larger domains that are fewer in number, thus reflecting an increase in the relative importance of coalescence.

The Jordhamo equation [29], an empirical relationship between the viscosity and the volume fractions of the two

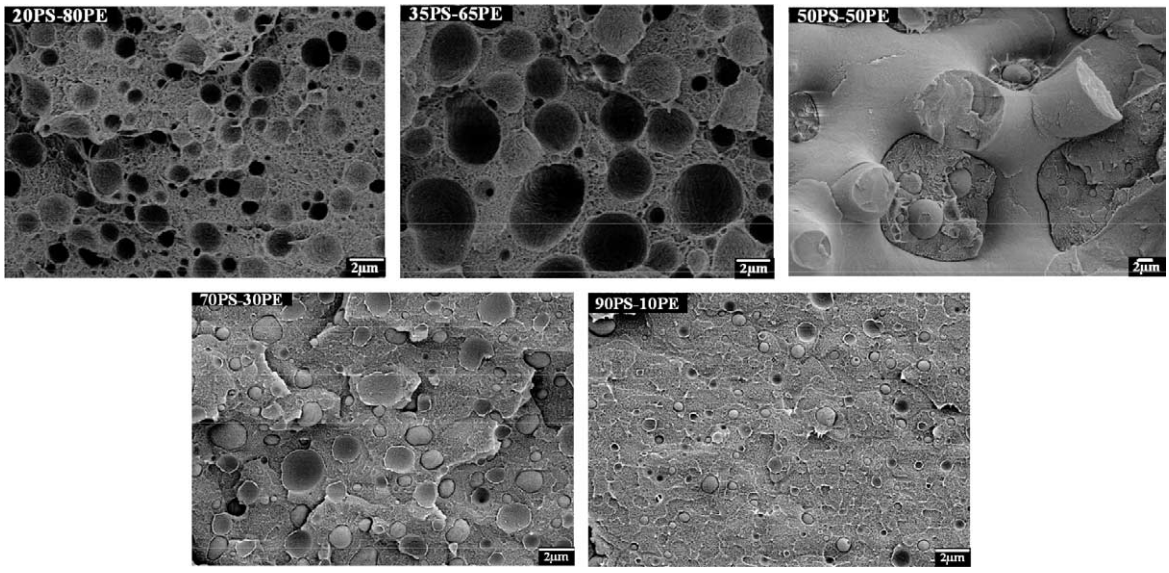

Fig. 1. SEM micrographs of PS–PE blend morphology at different compositions, (a) 20PS–80PE, (b) 35PS–65PE, (c) 50PS–50PE, (d) 70PS–30PE, (e) 90PS–10PE.

phases at process shear and temperatures, predicts co-continuity at about 50PS/50PE for these blends. The micrograph for the 50/50 composition suggests a co-continuous structure, illustrating a configuration in which both phases surround each other. The size of the PS domains has increased significantly from that in 35PS/65PE. The other end of the composition spectrum, 70PS/30PE and 90PS/10PE, shows PE dispersed in the PS matrix with finer domain dimensions compared to the 50/50 composition.

Fig. 2 shows the cross-sectional view of the extruded PS–PP samples. The compositional variation of morphology is very similar to the PS/PE blends with the 15PS/85PP and 30PS/70PP blends consisting of PS dispersed in a PP matrix. The co-continuous structure is observed at 50PS/50PP, and a PP dispersed in PS structure appears at the 70PS/30PP and 90PS/10PP compositions.

3.1.2. Glass transition

The effect of PS/PE blend compositions on the polystyrene glass transition temperatures as measured by DSC are shown in Fig. 3. The derivatives of the reversing heat curves are plotted for ease of glass transition detection, assignment and comparison. The data show an increase in PS T_g with decreasing PS concentration. The T_g of neat PS is approximately 104.8 °C, whereas the T_g of PS in the blends increases to 107.4 °C as its concentration decreases to 20%.

A monotonic and nearly linear increase in PS T_g over the composition range (Fig. 4) as PE is added to neat PS is observed. A remarkable feature of these results is that the T_g increase is observed over a wide range of morphologies, from PE dispersed in PS to co-continuous to PS dispersed in PE. To corroborate these findings, the PS T_g's in these blends were also measured by DMA (Fig. 5). The loss modulus (G'') curves

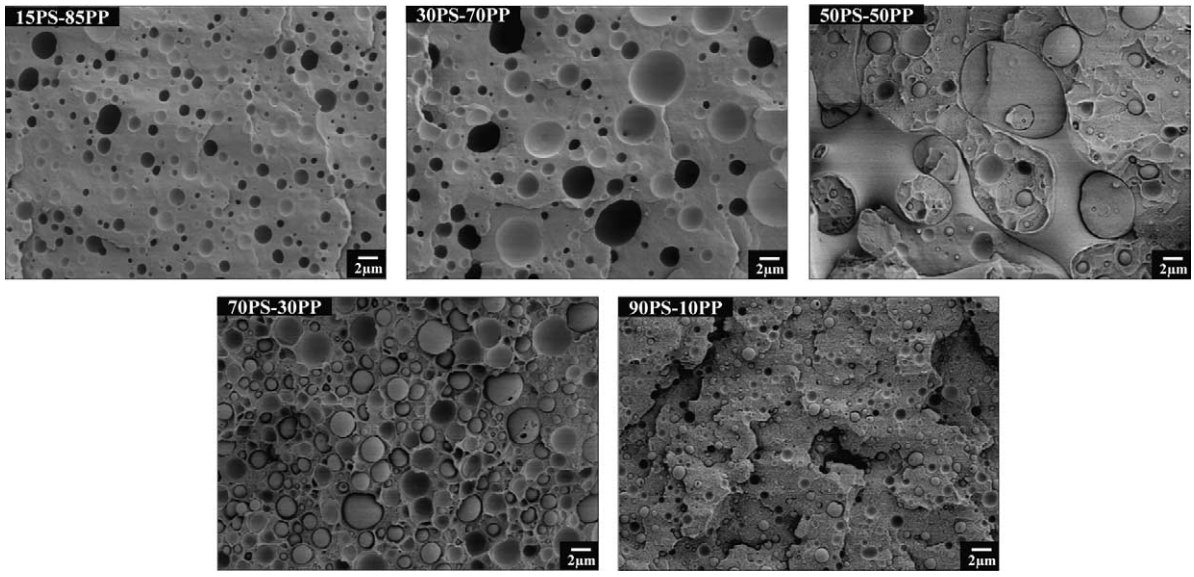

Fig. 2. SEM micrographs of PS–PP blend morphology at different compositions, (a) 15PS–85PP, (b) 30PS–70PP, (c) 50PS–50PP, (d) 70PS–30PP, (e) 90PS–10PP.

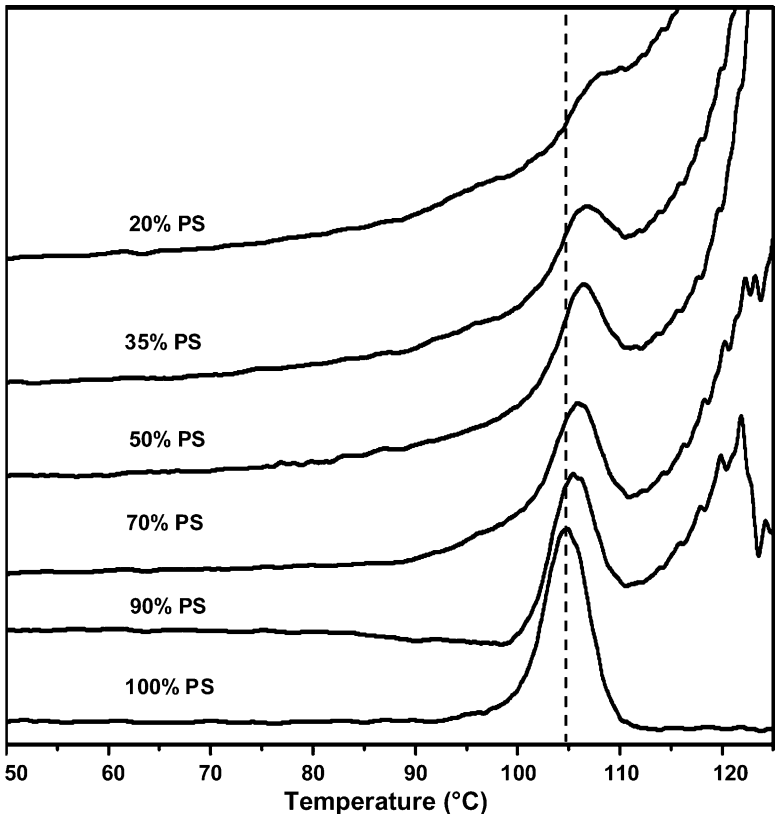

Fig. 3. Derivative of the DSC reversing heat flow curves showing PS T_g in PS/PE blends (peaks denote PS T_g; dotted line denotes 100% PS T_g).

for various compositions are plotted, and a trend in good agreement with that obtained from DSC data is observed. Interestingly the PE glass transition, which was also measured over the blend range using DMA and is displayed with the PS data (Fig. 6), also changes over this compositional range. The PE T_g is constant in the range (PS < 50%) where PE surrounds PS and/or is co-continuous with PS, but then decreases steadily as the PS concentration is increased above 50%.

With regard to PS/PP blends, the composition dependent T_g behavior shown in our earlier work was also observed in the PS/PP blends prepared for this work, i.e. the T_g of the amorphous polymer (PS) in the blend increases when blended with the semicrystalline polymer (PP) having T_c greater than the PS T_g of the amorphous material (Fig. 4) [22]. Although the T_g-composition relationship is similar to that observed for the PS/PE system at low PS concentrations, the rate at which the T_g changes with small PP additions to bulk PS is different from the PS/PE system. Indeed, the T_g of the 70/30 PS/PP blend is 104.8 °C, virtually unchanged from the value for the 100% PS. For PS compositions less than 70%, the T_g values show an increase with composition similar to that observed in PS/PE blends. DMA analyses of these blends (Fig. 7) confirm this behavior.

The well-known PS/PE and PS/PP blend systems are immiscible, due in part to their semicrystalline nature and in part to entropy restrictions of mixing high molecular weight polymers. Furthermore, the solubility parameter difference between PS and PP/PE is additional evidence of the thermodynamic immiscibility of these blends. The observed shift in glass transition values is not expected in these blends as such variations are normally observed in partially or fully miscible blends, where miscibility generates a smooth variation in T_g over composition. More importantly, if PS/PE and PS/PP were miscible blends, the PS T_g would be expected to decrease and move towards the T_g of PE or PP as given by the rule of mixtures behavior commonly seen in miscible systems. Moreover, the glass transition of PP (~3 °C) in the blends studied, as measured by DMA, did not change and

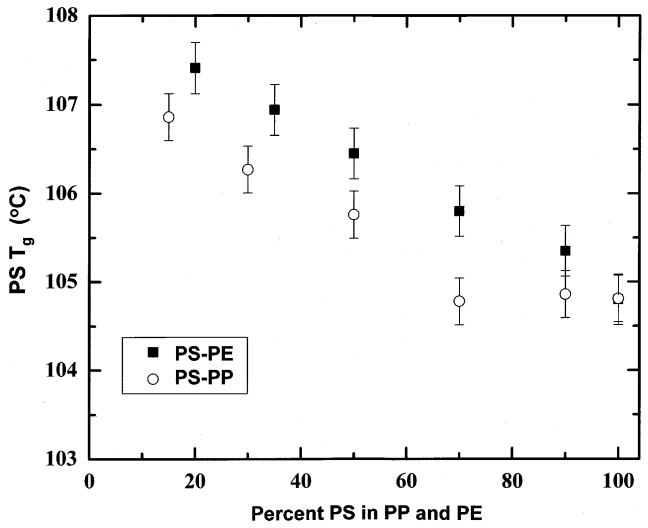

Fig. 4. Polystyrene T_g as a function of blend composition in PS/PE and PS/PP blends. Error bars are $\mu \pm t_{(p=0.05)}\sigma_\mu$.

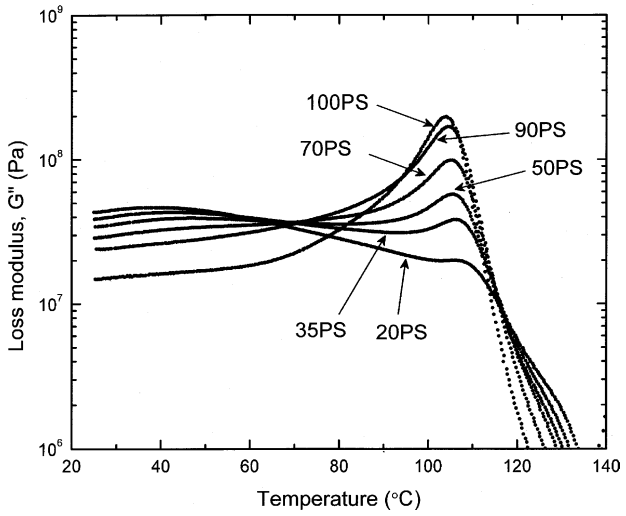

Fig. 5. DMA loss modulus curves showing PS T_g in PS/PE blends.

remained essentially constant over the entire composition range (Fig. 8).

3.1.3. Mechanisms—low PS compositions

Glass transition shifts in the PS/PE and PS/PP blends can be explained based on the physical interactions between the components, an effect shown most dramatically in the PS/PP blends. The 15PS/85PP and 30PS/70PP blends clearly show morphologies in which PP completely surrounds the PS phase, whereas the co-continuous structure of 50PS/50PP includes a partial surrounding of PS by the PP phase. The highest T_g value is observed in the 15PS/85PP blend and the values decrease with increasing PS until the 50PS/50PP blend is reached. From that point, there is no statistically significant change in PS T_g with composition with further increases in PS concentration. Thus, the T_g data (Fig. 4) can be interpreted as consisting of two regimes, less than and greater than 70% PS. Correlation of the T_g values with the morphology suggests that the PS T_g increases only when the PS phase is surrounded by the PP phase, whereas the regions in which the PS is not surrounded

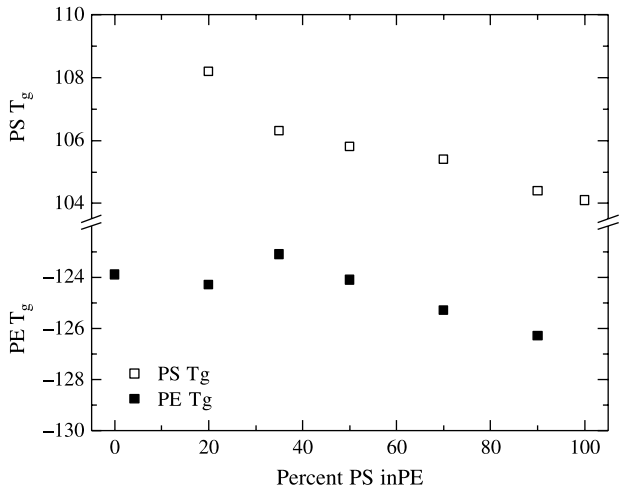

Fig. 6. DMA loss modulus curves showing PE T_g in PS/PE blends.

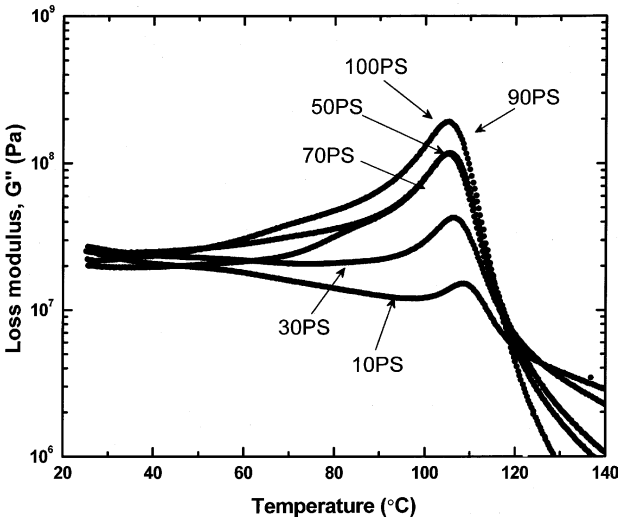

Fig. 7. DMA loss modulus curves showing PS T_g in PS/PP blends.

by PP (PS surrounds PP) the T_g remains unchanged and maintains the bulk PS T_g value.

The PS/PE blends demonstrate similar variations in T_g with composition when PS is surrounded by the semicrystalline PE, i.e. the co-continuous composition and compositions with lower PS concentrations, but is different at higher PS concentrations where PE consists of dispersed domains surrounded by PS, i.e. 70% PS and 90% PS compositions. The high values of the polystyrene T_g at the low PS compositions can be understood by considering the dynamics of the phases during cooling from the melt state. Crystallization of the PE phase corresponds to the movement of the macromolecular chains towards an ordered, denser structure from the entangled mass of disordered, mobile chains at the melt temperature. This crystallization process, which occurs to a high degree in PE, generates significant volume reduction and shrinkage, much more so than occurs during cooling of the amorphous polystyrene domains. Polyethylene crystallizes at 120 °C, at

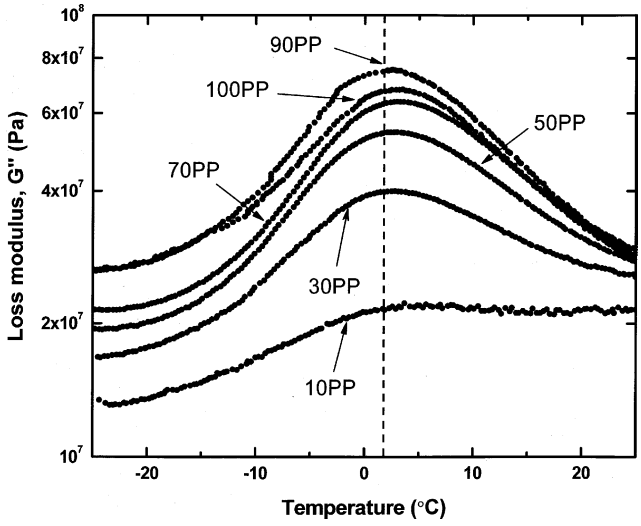

Fig. 8. DMA loss modulus curves showing PP T_g in PS/PP blends (dotted lines indicates 100% PP T_g).

which temperature polystyrene is a liquid above T_g. The differential shrinkage causes the PE phase to exert isotropic pressure on the liquid polystyrene phase and of course the polystyrene liquid applies an equal and opposite pressure on the polyethylene. As cooling continues the dispersed PS liquid undergoes T_g at a temperature elevated relative to the bulk T_g of PS due to the well known pressure dependence of the glass transition [30]. The free volume theory of glass transition cites the lack of free volume between the polymer chains as the causative factor for the pressure dependence of T_g. When pressure is applied to liquid polystyrene, the available free volume is reduced, the ability of the polymer chains to conform to the normal low temperature configuration (critical free volume) is constrained, and as a result the glass structure is attained at a higher temperature. Thus, the increase in PS T_g in a PE matrix via isotropic clamping stresses is explained for the instances where PE fully surrounds PS.

In the 20PS/80PE blend the spacing between the PS domains is large owing simply to the low concentration of PS. Thus, from a qualitative mechanics perspective, it seems reasonable to assume that each PS domain can be considered to be surrounded by an infinite amount of PE, i.e. the pressure effects mentioned above for one PS domain do not affect a neighboring PS domain. Hence, each PS sphere can be modeled as existing in an infinite PE matrix, with the effect of pressure exerted by PE on one PS sphere being independent of the other one. This situation changes as the PS composition is increased to 35%. The inter-particle distance between the dispersed PS spheres decreases due to the increasing concentration of PS. Thus, the assumption that the PS spheres are in an infinite PE matrix is not valid and the PE shrinkage is distributed over a greater number of PS spheres, reducing the magnitude of the isotropic pressure in the PS domains and reducing the degree of T_g elevation.

An initial quantitative estimate was made of the approximate magnitude of pressure applied on the dispersed PS phase by the shrinking semicrystalline phase at the lowest PS compositions in PS/PP and PS/PE blends. Using the pressure dependence of atactic PS T_g calculated by Stevens et al. [31], the increase in pressure (ΔP) required for a T_g elevation of 2.10 °C in PS/PP (15PS/85PP composition) and 2.56 °C in PS/PE (20PS/80PE composition) was calculated. Such pressures, applied on the dispersed PS by the surrounding semicrystalline polymer, are estimated at 6.8 MPa in PS/PP and 8.7 MPa for PS/PE. These values are considerably lower than the yield stress of the polymers and hence such stresses will be entirely within the proportional elastic limit.

3.1.4. Mechanisms—co-continuous blends

The blend morphology transitions from dispersed to co-continuous as the PS composition increases from 35 to 50%. The co-continuous structure consists of a morphology in which both phases surround each other and both phases are continuous. Such structures, in theory, consist of only two large polymer domains, one of PS and one of PE, both extending completely through the structure. The co-continuous morphology is characterized by domain branching and domain boundaries that frequently change curvature both with respect to magnitude and sign. Thus, the isotropic pressure model becomes more complicated and depends on these two factors. Broadly, when the curvature of the interface is positive with respect to the position of PS, the PE shrinks away from the PS upon cooling and either exerts tension on the PS or becomes a non-contacting interface. When the curvature of the interface is negative with respect to the position of PS, the PE contracts around the PS and provides the compressive stress discussed above for systems of dispersed PS in PE. Hence, the 50% PS blend has a lower T_g than the previous two compositions (20 and 35%) since a portion of the polystyrene is not surrounded by PE and thus not under compressive pressure. This is a difficult modeling regime and there are elements of the behavior that are not well understood. For example, one might expect to observe two T_g's in this region since some of the PS is under compression and some is not. Only one T_g is observed. Alternatively, since the phases are co-continuous and the PS is a liquid when the PE is cooled through its crystallization temperature, some of the liquid PS may extrude through co-continuous bottlenecks to partially equalize isotropic pressure, although the viscosity of the PS at these temperatures is high and cooling times are short.

3.1.5. Mechanisms—high PS compositions

At blend compositions greater than 50% PS a more complicated relationship exists between the two phases, wherein the T_gs of both PS and PE change nearly in parallel (Fig. 6). Clearly some process occurs between the two phases such that, as small volumes of PE are added to neat PS, the T_g of the PS increases as does the T_g of the small, dispersed domains of PE. We note that although both T_gs are increasing from right to left in Fig. 6, the PS T_g is increasing above the T_g of the neat polymer whereas the T_g of the PE is increasing from a depressed PE T_g towards the value of the neat PE. Since both T_g's increase in parallel, the effect is not likely generated by the diffusion of a mutually soluble T_g-reducing component from one phase to another. T_g shifts arising from the presence of a thermally-induced tensile stress between the matrix PS and the dispersed PE domains can also be eliminated from consideration since the immiscible interfaces are weakly bonded and the likelihood of significant tensile stresses is low. In any event, such tensile stresses would lower the T_g of both phases, counter to observed fact. A physical model by which limited domain size generates higher T_g's upon cooling of the melt owing to conformational constraints in small domains is a possible explanation. However, the domain sizes in these blends are not particularly small, especially the PS domains at the PS-rich end of the compositional range. Perhaps a more probable mechanism in this environment is similar to that associated with observed T_g effects in polypropylene, Nylon-6 [15] and polystyrene [17], melt blended with inorganic glass bead fillers and in nanocomposites of polymers filled with inorganic nanoparticles [11]. In these environments, the presence of a solid surface interface in contact with PS during the glass transition process results in the creation of an immobile polymer interfacial layer at the inorganic filler surface, which constrains the PS during

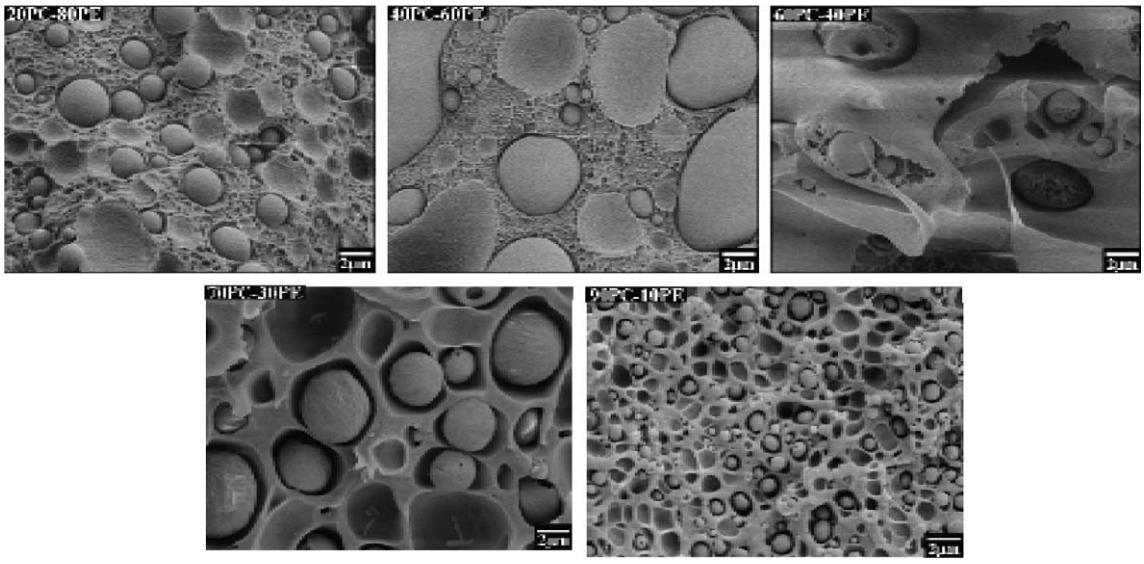

Fig. 9. SEM micrographs of PC–PE blend morphology at different compositions, (a) 20PC–80PE, (b) 40PC–65PE, (c) 60PC–50PE, (d) 80PC–30PE.

cooling and prevents conformation to low free volume configurations, thus resulting in elevated glass transition temperatures. The presence of semicrystalline PE in the PS melt may be serving a similar function and preventing PS from thermally relaxing and conforming to a bulk PS T_g, although this mechanism does not account for the PE T_g behavior.

3.2. PC–PE blends

From the perspective of image analysis and morphology (Fig. 9) blends prepared from PC and PE are similar to the other blends in this study in that they show three distinct regions of phase distribution over the composition range. The average PC domain size in the 20PC/80PE composition is about 2 μm. In the 40PC/60PE composition, the PC phase has increased in size and changed from a spherical morphology to an elongated, oriented structure. Co-continuous type of morphology is observed in the 60PC/40PE blend, consistent with the Jordhamo predicted approximate composition for co-continuity at 65PC/35PE. Well-dispersed spheres of PE in the PC matrix are observed in the 70PC/30PE and 90PC/10PE compositions. The dispersed PE phase has pulled away from the PC matrix during crystallization, due to the differential shrinkage and incompatibility between PC and PE. The rationale behind exploring these blends was to change the sequence of the crystallization of the semicrystalline component and the glass transition of the amorphous component of the blend. In the PC/PE system, the glass transition of the amorphous component (PC) occurs in the presence of a liquid phase (PE), a direct reversal of the conditions experienced by PS in PE. Such a system, therefore, provides a useful contrast to the microstructural mechanics of the cooling-induced morphologies in the PS/PE and PS/PP systems.

The PC T_g in the PC/PE blends is constant with composition (Figs. 10 and 11) and does not reflect the composition dependence identified in the PS/PE and PS/PP systems. The data in Fig. 10 are the reversing heat flow component of reheat MDSC analyses and Fig. 11 graphs the 3-fold replication of the T_g values on a composition axis. These data are the derivatives of the reversing heat curves. The value of pure polycarbonate T_g is about 150 °C and the T_g values for the blend compositions show some scatter around 150 °C, but none is statistically different from the mean value ($lsd_{(p=0.05)}=0.5$ °C) and therefore, no compositional dependence exists. The DSC results of the PC glass transition values are verified with the DMA results and are shown in Fig. 12, which again show compositional independence of the T_g values. Such behavior is traditionally expected since PC and PE are known to be highly incompatible. However, these results become more interesting in light of the PS–PE results where PS T_g changed over the blend composition range in what is also a highly immiscible

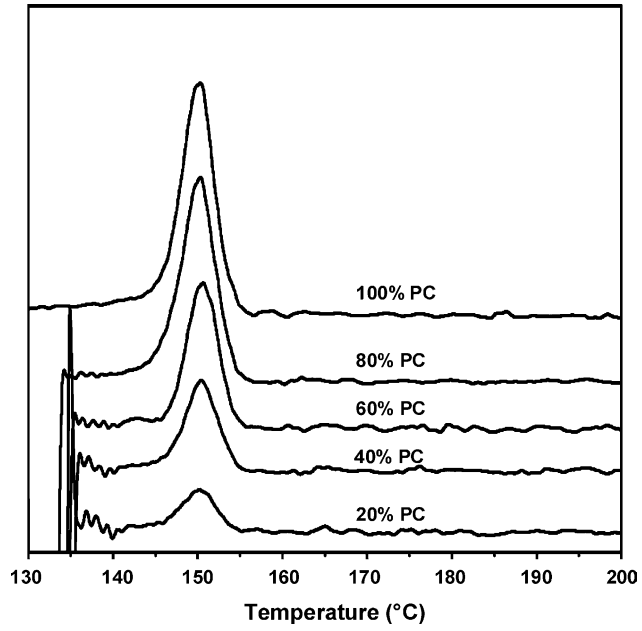

Fig. 10. Derivative of the DSC reversing heat flow curves showing PC T_g in PC/PE blends.

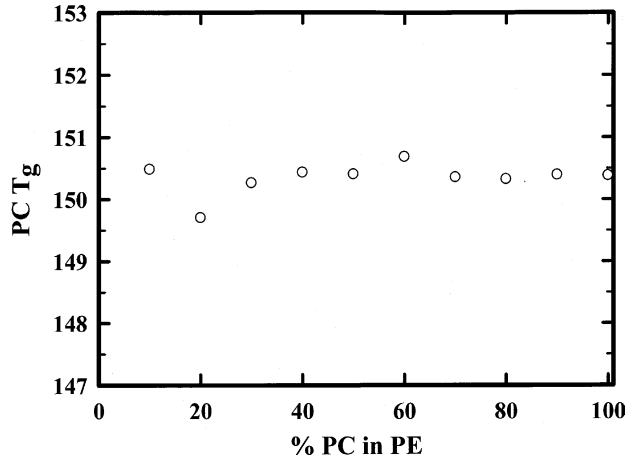

Fig. 11. Polycarbonate T_g as a function of blend composition in PC/PE blends.

system. Consider the 20PC/80PE and 40PC/60PE blends, where PC is dispersed in a PE matrix. The PC T_g in both compositions occurs at 150 °C, with the onset at 145 °C. During this transition, the surrounding PE phase is in liquid form, a point of principal contrast between these blends and PS/PE system. Since, PE is a liquid at the temperature at which PC transitions to a glassy phase, the T_g of the PC is unaffected since no compressive stresses are present. This behavior is in sharp contrast to PS/PE blends where PE crystallization and shrinkage results in PS compression and an increase in PS T_g.

The blends with high PC concentrations also do not reveal a change in PC T_g from the neat PC value. This is somewhat similar to the high PS compositions in PS/PP blends where composition dependence was strong at low PS concentrations but was virtually nil at high PS compositions. However, this behavior is unlike the PS/PE blends where significant T_g shifts were observed even at very low PE compositions. The reason that PS/PE behaves differently compared to PC/PE is not clear but may relate to the physical state of the semicrystalline phase during the glass transition or a yet unidentified chemical interaction between the domains.

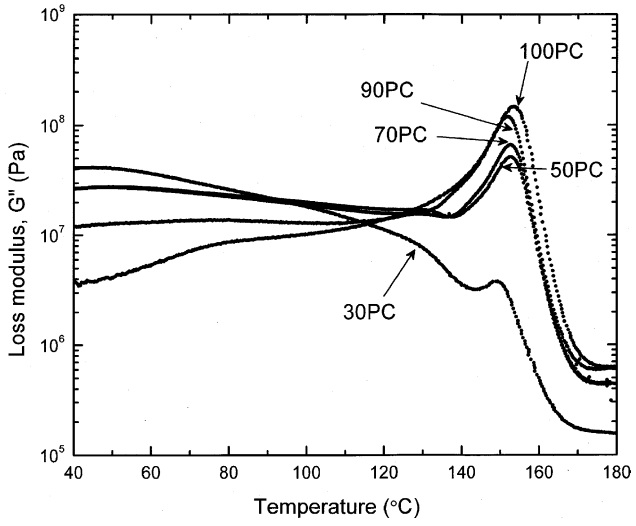

Fig. 12. DMA loss modulus curves showing PC T_g in PC/PE blends.

4. Summary and conclusions

Immiscible blends of an amorphous polymer, PS, and two semicrystalline polymers, PP and PE, were prepared through melt compounding. A variety of morphologies were observed over the compositional range of these blends, ranging from dispersed structures near the neat polymer compositions to co-continuous structures near the phase inversion point. Although these polymers are widely regarded as completely immiscible, the glass transition temperatures of PS in both the blends, PS/PP and PS/PE, varied as a function of the composition, thus indicating some type of composite interaction. The T_g values of PS increased with decreasing PS concentration in these blends. In PS/PP blends, the PS T_g increased with decreasing PS only in compositions containing 50% PS or less, whereas the T_g increased with decreasing PS throughout the composition spectrum for PS/PE blends. The tendency of PS T_g to increase in these blend systems represents a shift opposite to that which would be expected if parts of the constituent polymers were miscible. Furthermore, in PS/PP blends the T_g of PP did not change with composition, suggesting that the phase interactions were physical, not chemical, and are dependent on changes in morphology that accompany the composition changes. The PS/PP blend data clearly show that the T_g increase is restricted to compositions in which the PP phase surrounds the PS phase either partially or completely. The cause for this behavior is compressive pressure exerted on the amorphous PS domains due to differential shrinkage between the amorphous PS and crystallizing PP. In PS/PE blends T_g shifts were observed in compositions greater than 50% PS, where PS surrounds PE, as well as in the lower PS concentration range. The increase in PS T_g at high PS concentrations, is accompanied by a parallel increase in PE T_g and may indicate an interaction between the amorphous component of the PE phase and the PS phase. Such an effect was only observed in PS/PE blends and may be specifically associated with this blend system. The tendency of the PS T_g to increase when low concentrations of PE are dispersed in the blend structure is not fully understood, but may result from immobilization of the polymer interfacial layer at the domain boundaries in a process similar to that observed in inorganic filled composite systems. Composition dependent glass transition behavior was not observed in PC/PE blends where, upon cooling, the PC glass transition occurs prior to the crystallization of the PE, thus eliminating the possibility of PE compression effects on the PC T_g.

References

[1] Utracki LA. Polymer alloys and blends: thermodynamics and rheology. 1st ed. Munich: Hanser; 1989.
[2] Hara M, Sauer JA. J Macromol Sci, Rev Macromol Chem Phys 1998;C38: 327–62.
[3] Joshi J, Lehman RL, Nosker TJ. J Appl Polym Sci 2005;99:2044–51.
[4] Nosker TJ, Morrow DR, Renfree RW, VanNess K, Donaghy JJ. Nature 1991;350.
[5] Donth E. The glass transition: relaxation dynamics in liquids and disordered materials. 1st ed. New York: Springer Verlag; 2001.

[6] Adam G, Gibbs JH. J Chem Phys 1965;43:139–46.
[7] Jackson CL, McKenna GB. Chem Mater 1996;8:2128–37.
[8] Forrest JA, Dalnoki-Veress K, Stevens JR, Dutcher JR. Phys Rev Lett 1996;77:2002–5.
[9] Forrest JA, Dalnoki-Veress K, Dutcher JR. Phys Rev E 1997;56:5705–16.
[10] van Zanten JH, Wallace WE, Wu W-I. Phys Rev E 1996;53:2053–6.
[11] Hergeth W-D, Steinau U-J, Bittrich H-J, Simon G, Schmutzler K. Polymer 1988;30:254–8.
[12] Ash B, Siegel RW, Shcadler LS. J Polym Sci, Part B: Polym Phys 2004; 42:4371–83.
[13] Ash BJ, Siegel RW, Schadler LS. Macromolecules 2004;37:1358–69.
[14] Bansal A, Yang H, Li C, Cho K, Benicewicz BC, Kumar SK, et al. Nat Mater 2005;4:693–8.
[15] Huang L, Yuan Q, Jiang W, An L, Jiang S, Li RKY. J Appl Polym Sci 2004;94:1885–90.
[16] Yuan Q, Jiang W, An L, Li RKY. Polym Adv Technol 2004;15:409–13.
[17] Ilsaka K, Shibayama K. J Appl Polym Sci 1978;22:3135–43.
[18] Mucha M. Colloid Polym Sci 1986;264:859–65.
[19] Reinsch VE, Rebenfeld L. J Appl Polym Sci 1996;59:1913–27.
[20] Greco R, Astarita MF, Dong L, Sorrentino A. Adv Polym Technol 1994; 13:259–74.
[21] Bates FS, Cohen RE, Argon AS. Macromolecules 1983;16:1108–14.
[22] Thirtha VM, Lehman RL, Nosker TJ. Polym Eng Sci 2005;45:1187–93.
[23] Wenig W, Fiedel HW, Scholl A. Colloid Polym Sci 1990;168:528–35.
[24] Everaert V, Aerts L, Groeninckx G. Polymer 1999;40:6627–44.
[25] Yin J, Wang S, Zhang Y, Zhang Y. J Polym Sci, Part B: Polym Phys 2005; 43:1914–23.
[26] Yuan Q, Jiang W, An L, Li RKY. J Polym Sci, Part B: Polym Phys 2004; 43:306–13.
[27] Santana OO, Muller AJ. Polym Bull 1994;32:471–7.
[28] Sundararaj U, Macosko CW. Macromolecules 1995;28:2647–57.
[29] Jordhamo GM, Mason JA, Sperling LH. Polym Eng Sci 1986;26:517–24.
[30] Ferry JD. Viscoelastic properties of polymers. 3rd ed. New York: Wiley; 1980.
[31] Stevens JR, Coakley RW, Chau KW, Hunt JL. J Chem Phys 1986;84: 1006–14.